Elliptic flow at RHIC: where and when does it formed?

L.V. Bravina [a,b] K. Tywoniuk [a] E.E. Zabrodin [a,b] G. Burau [c]
J. Bleibel [c] C. Fuchs [c] Amand Faessler [c]

[a] *Department of Physics, University of Oslo, Blindern 1048, N-0316 Oslo, Norway*

[b] *Skobeltzyn Institute for Nuclear Physics, Moscow State University, Vorobievy Gory, RU-119899 Moscow, Russia*

[c] *Institute for Theoretical Physics, University of Tübingen, Auf der Morgenstelle 14, D-72076 Tübingen, Germany*

Abstract

Evolution of the elliptic flow of hadrons in heavy-ion collisions at RHIC energies is studied within the microscopic quark-gluon string model. The elliptic flow is shown to have a multi-component structure caused by (i) rescattering and (ii) absorption processes in spatially asymmetric medium. Together with different freeze-out dynamics of mesons and baryons, these processes lead to the following trend in the flow formation: the later the mesons are frozen, the weaker their elliptic flow, whereas baryon fraction develops stronger elliptic flow during the late stages of the fireball evolution. Comparison with the PHOBOS data demonstrates the model ability to reproduce the $v_2^{ch}(\eta)$ signal in different centrality bins.

Key words: ultrarelativistic heavy-ion collisions, elliptic flow, freeze-out of particles, Monte-Carlo quark-gluon string model
PACS: 25.75.-q, 25.75.Ld, 24.10.Lx

1 Introduction

Elliptic flow is defined as the second harmonic coefficient v_2 of an azimuthal Fourier expansion of the particle invariant distribution [1]

$$E\frac{d^3N}{d^3p} = \frac{1}{\pi}\frac{d^2N}{dp_t^2 dy}\left[1 + 2v_1\cos(\phi) + 2v_2\cos(2\phi) + \ldots\right] , \qquad (1)$$

where ϕ is the azimuthal angle between the transverse momentum of the particle and the reaction plane, and p_t and y is the transverse momentum and

the rapidity, respectively. The first harmonic coefficient v_1 is called directed flow. It can be presented as

$$v_1 \equiv \langle \cos\phi \rangle = \left\langle \frac{p_x}{p_t} \right\rangle \ , \tag{2}$$

while the v_2, which measures the eccentricity of the particle distribution in the momentum space, is

$$v_2 \equiv \langle \cos 2\phi \rangle = \left\langle \frac{p_x^2 - p_y^2}{p_t^2} \right\rangle \ . \tag{3}$$

(Note, that in the coordinate system applied the z-axis is directed along the beam, and the impact parameter axis is labeled as x-axis. Therefore, transverse momentum of a particle is simply $p_t = \sqrt{p_x^2 + p_y^2}$).

The overlapping area of two nuclei colliding with non-zero impact parameter b has a characteristic almond shape [2] in the transverse plane. The fireball tries to restore spherical shape, provided the thermalization sets in rapidly and the hydrodynamic description is appropriate [3,4,5,6]. When it becomes spherical, apparently, the elliptic flow stops to develop. Therefore, v_2 can carry important information about the earlier phase of ultrarelativistic heavy-ion collisions, equation of state (EOS) of hot and dense hadronic (or rather partonic) matter, and is expected to be a useful tool to probe the formation and hadronization of the quark-gluon plasma (QGP) [7].

Elliptic flow of charged particles was among the first signals measured at Relativistic Heavy Ion Collider (RHIC) in Brookhaven [8], and now there is plenty of data concerning the centrality, the (pseudo)rapidity, and, especially, the transverse momentum dependence of the v_2 in gold-gold collisions at $\sqrt{s} = 130$ AGeV [9] and at $\sqrt{s} = 200$ AGeV [10]. Microscopic models based on string phenomenology and transport theory are able to reproduce, at least qualitatively, many features of the v_2 at ultrarelativistic energies [11,12,13,14,15,16,17,18], however, the quantitative agreement with the data is often not so good. Particularly, magnitude of the distributions $v_2(\eta)$ or $v_2(p_t \geq 1.5\,\mathrm{GeV}/c)$ appears to be too high. Does it mean that the effective EOS of hot and dense partonic-hadronic matter in microscopic models is too soft? What should be done to match the data? Before starting our study it is worth noting that the elliptic flow increases due to two main processes, namely, (i) elastic or inelastic rescattering of particles, and (ii) non-homogeneous absorption of particles in spatially asymmetric dense medium. The first reaction is responsible for the formation and development of the hydrodynamic flow, while the latter one should be considered as a non-hydro contribution.

Then, the microscopic calculations [19,20,21,22] show the absence of sharp freeze-out of particles in relativistic heavy-ion collisions. In contrast to assumptions of hydrodynamic model [23], the expanding fireball in microscopic models can be rather treated as a core consisting of still interacting hadrons, and a halo, which contains particles already decoupled from the system. The order of the freeze-out of different species seems to be the same for energies ranging from AGS to RHIC: 1 - pions, 2 - kaons, 3 - lambdas, 4 - nucleons. What are the consequences of the continuous freeze-out for the v_2 of these particles? What is the role of the rescattering and absorption in the flow development? When (and where) the elliptic flow is formed?

2 Model

To answer these questions we employ the quark-gluon string model (QGSM) [25,26], which is a microscopic model based on the Gribov-Regge theory [24] of hadronic and nuclear interactions at high energies. The main advantage of the GRT is the fulfillment of unitarity conditions in s- and t-channel for multiparticle processes. On one hand, the Regge-pole exchange in t-channel determines two-particle amplitude at $s \to \infty$. On the other hand, Regge-pole exchanges fully determine multiparticle processes in s-channel, since each Regge-pole exchange in t-channel corresponds to a jet of hadrons with small transverse momenta. Therefore, unitarity is fulfilled. In the QGSM the subprocesses with quark annihilation and quark exchange correspond to the so-called Reggeon exchange in two-particle amplitudes in the GRT, while the subprocesses with colour exchange are represented by the one and more Pomeron exchanges in elastic amplitudes. This scheme is closely related to that given by the partonic model, where most of calculations imply somehow calculation of contributions of diagrams arising in the GRT. More information concerning the link between the GRT and quantum chromodynamics (QCD) can be found, e.g., in [24,27,28,29] and references therein.

Note also, that number of scattering partons (partonic density) within hadrons or nuclei, colliding at ultrarelativistic energies, increases with the rise of center-of-mass energy $\sqrt{s}$ as $s^{n[\alpha_P(0)-1]}$ with $\alpha_P(0) > 1$ being the intercept of a Pomeranchuk pole. This leads to the transition to Froissart regime corresponding to multiparton collision of black disks filled out by slow partons, i.e., the state which is a precursor of the Color Glass Condensate (see, e.g., [30] and references therein). The QGSM incorporates also the string fragmentation, resonance formation, and hadronic rescattering. The latter implies that the decay products of a string, - stable hadrons and their resonances, - can further interact with other hadrons. Due to uncertainty principle, secondary hadrons are allowed to interact again only after certain formation time, but hadrons containing the valence quarks of the colliding hadrons/nuclei can interact im-

mediately with the reduced cross section σ_{qN} taken from the additive quark model. Angular and momentum distributions of secondaries are adjusted to available experimental data. In addition, the one-pion exchange model, detailed balance constructions, and isospin symmetry arguments are used in case of lacking the experimental information. The positions and momenta of nucleons inside the colliding nuclei are Monte Carlo generated according to the Woods-Saxon density distribution and the Fermi momentum distribution, respectively. The Pauli blocking is taken into account by excluding the scattering into occupied final states.

The transverse motion of hadrons in the QGSM arises from different sources: (i) primordial transverse momentum of the constituent quarks, (ii) transverse momentum of (di)quark-anti(di)quark pairs acquired at string breakup, (iii) the transverse Fermi motion of nucleons in colliding nuclei, and (iv) rescattering of secondaries. Parameters of the first two sources are fixed by comparison with hadronic data. The Fermi motion changes the effective transverse distribution of strings formed by the valence quarks and diquarks of the target and projectile nucleons. Thus, the original strings are not completely parallel to the beam axis. Further details of the QGSM can be found elsewhere [25,26].

3 Development of elliptic flow

To investigate the development of the elliptic flow ca. $20{\cdot}10^3$ gold-gold collisions with the impact parameter $b = 8$ fm were generated at $\sqrt{s} = 130$ AGeV. According to previous studies [8,11] the elliptic flow of charged particles is close to its maximum at this impact parameter, and the multiplicity of secondaries is still quite high. The time evolutions of the v_2 of pions and nucleons as functions of rapidity

$$v_2(y) = \int_0^{p_t^{max}} \cos(2\phi) \frac{d^2N}{dydp_t} dp_t \Big/ \int_0^{p_t^{max}} \frac{d^2N}{dydp_t} dp_t \tag{4}$$

are displayed in Fig. 1(a). Here the snapshots of the v_2 profile are taken at 2 fm/c, 4 fm/c, ... 10 fm/c, and at the time of thermal freeze-out. This means that the hadronic composition was frozen at certain time $t = t_i$, when all interactions were switched off and particles were propagated freely. To avoid ambiguities, resonances were allowed to decay according to their branching ratios. Surprisingly, at $t = 2$ fm/c elliptic flow of pions is weak. The flow continuously increases and reaches its maximum value $v_2^{\pi}(y = 0) \approx 5\%$ already at $t = 6$ fm/c. From this time the elliptic flow does not increase anymore. Instead, it becomes broader and develops a two-hump structure with a relatively weak dip at midrapidity. The flow seems to continue development till the late stages

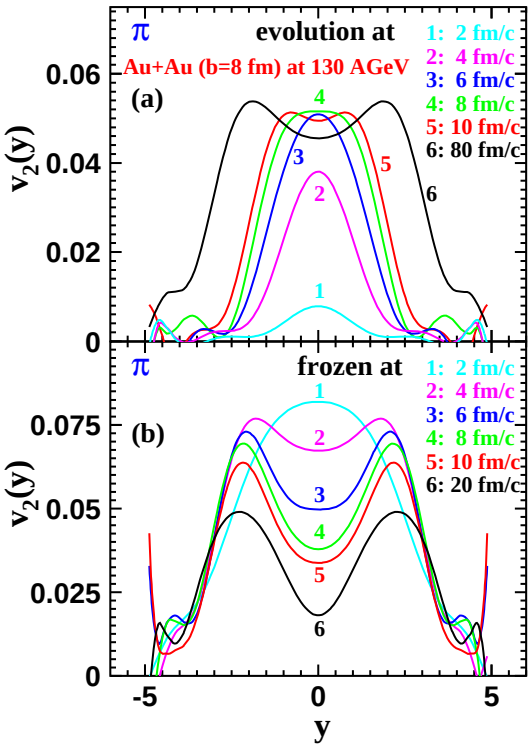

Fig. 1. Gold-gold collisions with $b = 8\,\mathrm{fm}$ at $\sqrt{s} = 130$ AGeV: (a) Evolution of elliptic flow of pions (snapshots are made at 2, 4, ... 80 fm/c), and (b) contributions to the resulting $v_2^\pi(y)$ coming from pions frozen at 2, 4, ... 20 fm/c, respectively.

of the system evolution. Bearing in mind the absence of sharp freeze-out of particles in model calculations, it is important to study the contribution of the survived particles to the resulting elliptic flow. The corresponding rapidity distributions presented in Fig. 1(b) reveal the peculiar feature: the v_2 of pions, which are frozen already at $t = 2$ fm/c, is the **strongest** among the fractions of the flow carried by pions decoupled from the fireball later on. The later the pions are frozen, the weaker their flow. The two-hump structure of the signal develops here as well, but the widths of all rapidity distributions are the same. For pions frozen after $t = 6$ fm/c the dip at midrapidity is seen quite distinctly. From here one can conclude that the strong elliptic anisotropy of pions, which left the system early, is caused by the absorption of the pion component in the squeeze-out direction.

For nucleons the evolution picture of the $v_2(y)$, shown in Fig. 2(a), is similar to that for pions. The flow is quite weak at $t = 2\,\mathrm{fm}/c$, then it increases and gets a full strength at midrapidity between $8\,\mathrm{fm}/c$ and $10\,\mathrm{fm}/c$, i.e. later than the elliptic flow of pions. Similarly to $v_2^\pi(y)$, it develops a two-hump structure, but the humps tend to dissolve at late stages of system evolution. In contrast to this behavior, the freeze-out decomposition picture of $v_2^N(y)$, presented in Fig. 2(b), does not show monotonic tendency within first $8\,\mathrm{fm}/c$ of the reaction: The flow of nucleons frozen at $2\,\mathrm{fm}/c$ is identical to that of nucleons frozen

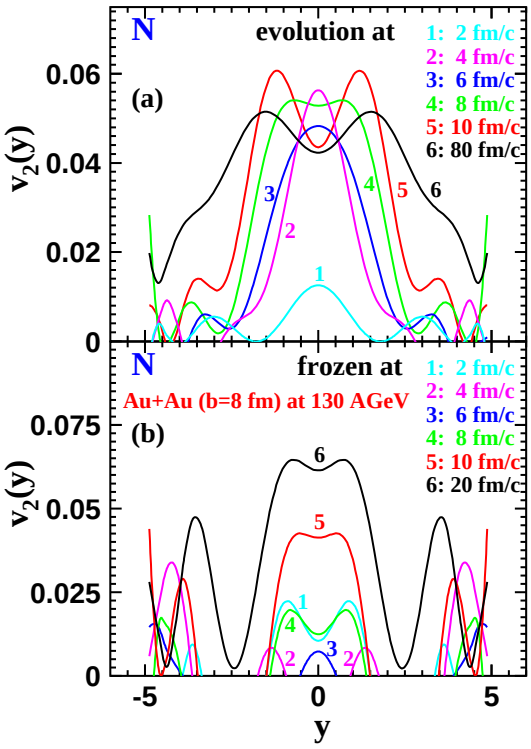

Fig. 2. The same as Fig.1 but for the elliptic flow of nucleons.

at 8 fm/c, whereas nucleons decoupled from the system between 2 fm/c and 8 fm/c almost do not contribute to the resulting elliptic flow. Nucleons, which are decoupled after 8 fm/c, have significant anisotropy in the momentum space, and the time development of flow in the nucleon sector is opposite to that in the pion one. Namely, the later the nucleons are frozen, the **stronger** their elliptic flow.

To clarify the role of particle freeze-out for the formation and evolution of their elliptic flow, the dN/dt distributions of n_{ch}, π, N, and Λ, which are decoupled from the system after the last elastic or inelastic collision, are depicted in Fig. 3(a). Here two features should be mentioned. Firstly, a substantial part of hadrons leave the fireball immediately after their production within the first two fm/c, in stark contrast with heavy-ion reactions at AGS [19] and at SPS [20] energies. Secondly, compared to lower energies, the particle distributions at RHIC are peaking at earlier times. For instance, the pion distribution has maximum at t^{π}_{max} = 5-6 fm/c, while the distributions of baryons are broader due to large number of rescatterings shifting their maxima to later times, t^{B}_{max} = 10-12 fm/c (cf. $t^{\pi}_{max} \approx 10$ fm/c and $t^{B}_{max} \approx 18$ fm/c at both AGS and SPS energies).

Elliptic flow carried by these hadronic species is presented in Fig. 3(b). The baryonic and mesonic components are completely different: pions emitted from the surface of the expanding fireball within the first few fm/c carry

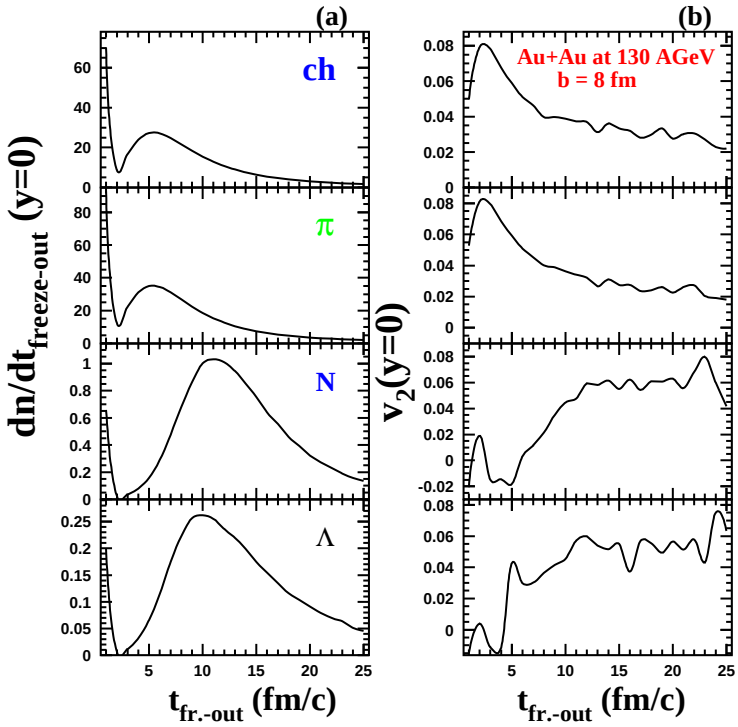

Fig. 3. (a) dN/dt distribution of n_{ch}, π, N, Λ over the time of their last interaction, and (b) elliptic flow of these particles for Au+Au collisions with $b = 8\,\mathrm{fm}$ at $\sqrt{s} = 130$ AGeV.

the strongest flow, while later on the flow of pions is significantly reduced. In contrast to pions, the baryon fraction acquires stronger elliptic flow during the subsequent rescatterings, thus developing the hydro-like flow. The saturation of the flow at the late stages can be explained by the lack of rescattering as the expanding system becomes more dilute, and by the restoration of the symmetry of particle momentum distributions in the transverse plane.

The flow has a multicomponent structure. In addition to hydrodynamic flow there are other components of the v_2 caused mainly by the particle splash from the surface area during the initial phase of nuclear collision, and by the non-uniform absorption of hadrons in spatially asymmetric dense matter. For instance, the anisotropic absorption of jets in x- and y-directions will contribute to the development of the elliptic flow of particles [31] with high transverse momenta. Hence, one may expect that the resulting elliptic flows of e.g. baryons and mesons obtained after the particle freeze-out are different. Figure 4 shows the rapidity dependence of the v_2 of most abundant particle species in Au+Au collisions at RHIC energies, namely pions, kaons, nucleons, and lambdas. Surprisingly, these distributions are almost indistinguishable: the widths and magnitudes of the signals are the same. To check the validity of the model calculations one has to perform more complex analysis of experimental data e.g. by studying the $v_2(y)$ distributions in different p_T-intervals. Other model

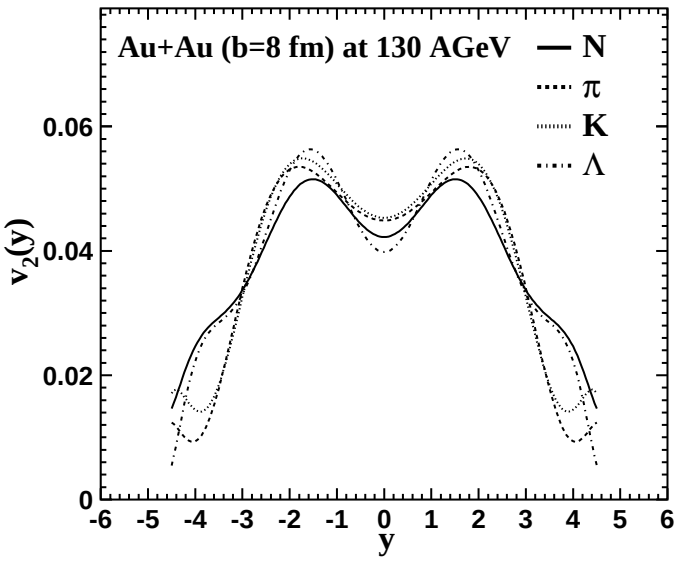

Fig. 4. Rapidity distribution of the resulting elliptic flow of nucleons (full line), pions (dashed line), kaons (dotted line), and lambdas (dash-dotted line) in Au+Au collisions with $b = 8\,\mathrm{fm}$ at $\sqrt{s} = 130$ AGeV.

predictions for the rapidity distribution of the elliptic flow of hadrons at both RHIC energies, 130 AGeV and 200 AGeV, can be found in [11,32,33,34]. Recently, PHOBOS collaboration presented the data on the $v_2(\eta)$ distributions of charged particles, produced in Au+Au collisions at 200 AGeV, in different centrality bins [35]. Model calculations are plotted onto the experimental results in Fig. 5. Here the elliptic flow of charged particles for the collisions with centralities 0-15% ($0\,fm \leq b < 2.3\,fm$), 15-25% ($2.3\,fm \leq b < 6.5\,fm$), and 25-50% ($6.5\,fm \leq b < 9.2\,fm$) is presented together with the resulting flow in minimum bias events. We see that the model reproduces the measured signal pretty well, including the nearly flat distribution at $|\eta| \leq 2$ and quick fall of the elliptic flow at $|\eta| \geq 2$. The only discrepancy appears to arise in semiperipheral collisions at midrapidity range, where the data are approximately 15% above the model results. This problem can be fixed by (i) the fine tuning of model parameters, and (ii) proper analysis of the experimental procedure of data handling (for the analysis and comparison of several methods applied to restore the anisotropic flow see [36]).

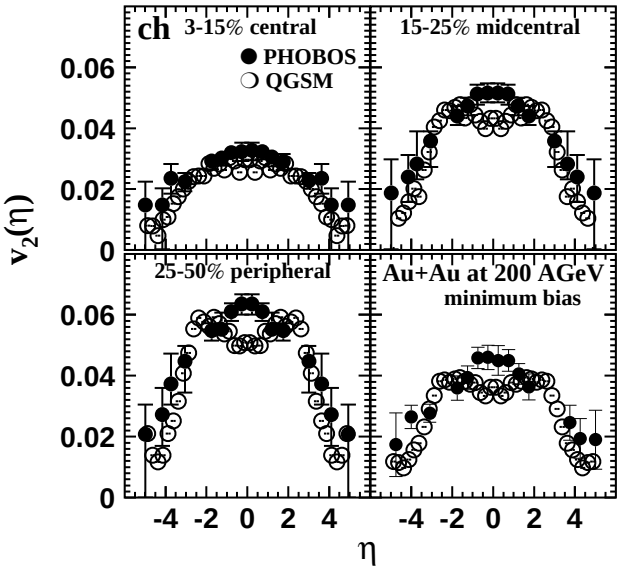

Fig. 5. $v_2(\eta)$ distribution of charged particles in Au+Au collisions at $\sqrt{s} = 200$ AGeV for (a) $\sigma/\sigma_{geo} = 0-15\%$, (b) $\sigma/\sigma_{geo} = 15-25\%$, (c) $\sigma/\sigma_{geo} = 25-50\%$, and (d) minimum bias events. Full symbols represent data [35], open symbols denote model calculations.

4 Conclusions

In summary, the features of the formation and development of elliptic flow in the microscopic quark-gluon string model can be stated as follows. First of all, there is no one-to-one correspondence between the apparent elliptic flow and the contribution to the final flow coming from the "survived" fraction of particles. For instance, apparent elliptic flow of pions at $t = 2$ fm/c is weak, but pions which are already decoupled from the system at this moment have the strongest elliptic anisotropy caused by the absorption of the pion component in the squeeze-out direction. Elliptic flow of hadrons is formed not only during the first few fm/c, but also during the whole evolution of the system because of continuous freeze-out of particles. Secondly, time evolutions of the mesonic flow and baryonic flow are quite different. Baryons, except of the fraction emitted within first two fm/c after the collision, are getting the stronger v_2 in the course of secondary interactions. Pions in average experience much less elastic collisions per particle because of their instant absorption and production in dense medium. As the substance becomes more dilute, their elliptic flow decreases. Freeze-out dynamics for baryons and mesons is also different, therefore, development of particle collective flow should not be

studied independently of the freeze-out picture. The general trend in particle flow formation in microscopic models at ultrarelativistic energies is that the earlier mesons are frozen, the weaker their elliptic flow. In contrast, baryons frozen at the end of the system evolution have stronger v_2.

Acknowledgments. Fruitful discussions with L. Csernai, R. Lacey, S. Panitkin, and S. Voloshin are gratefully acknowledged. This work was supported by the Norwegian Research Council (NFR) and by the Bundesministerium für Bildung und Forschung under contract 06TÜ986.

References

[1] S. Voloshin and Y. Zhang, Z. Phys. C 70 (1996) 665.

[2] H. Sorge, Phys. Rev. Lett. 78 (1997) 2309; *ibid.* 82 (1999) 2048.

[3] J.-Y. Ollitrault, Phys. Rev. D 46 (1992) 229; *ibid.* 48 (1993) 1132.

[4] A.M. Poskanzer and S.A. Voloshin, Phys. Rev. C 58 (1998) 1671.

[5] P.F. Kolb, J. Sollfrank, and U. Heinz, Phys. Rev. C 62 (2000) 054909; P.F. Kolb, P. Huovinen, U. Heinz, and H. Heiselberg, Phys. Lett. B 500 (2001) 232.

[6] D. Teaney, J. Lauret, and E.V. Shuryak, Phys. Rev. Lett. 86 (2001) 4783.

[7] Proc. of the Conf. Quark Matter'02 (Nantes, France, 2002) [Nucl. Phys. A 715 (2003) 1c]; Proc. of the Quark Matter'04 (Oakland, USA, 2004), [J. Phys. G 30 (2004) S1].

[8] K.H. Ackermann et al., STAR Collaboration, Phys. Rev. Lett. 86 (2001) 402.

[9] C. Adler et al., STAR Collaboration, Phys. Rev. Lett. 87 (2001) 182301; Phys. Rev. C 66 (2002) 034904; R.A. Lacey et al., PHENIX Collaboration, Nucl. Phys. A 698 (2002) 559; B.B. Back et al., PHOBOS Collaboration, Phys. Rev. Lett. 89 (2002) 222301; I.C. Park et al., PHOBOS Collaboration, Nucl. Phys. A 698 (2002) 564.

[10] P. Sorensen et al., STAR Collaboration, J. Phys. G 30 (2004) S217; S.S. Adler et al., PHENIX Collaboration, Phys. Rev. Lett. 91 (2003) 182301; S. Manly et al., PHOBOS Collaboration, Nucl. Phys. A 715 (2003) 611.

[11] E.E. Zabrodin, C. Fuchs, L.V. Bravina, and A. Faessler, Phys. Lett. B 508 (2001) 184.

[12] M. Bleicher and H. Stöcker, Phys. Lett. B 526 (2002) 309.

[13] H. Stöcker, E.L. Bratkovskaya, M. Bleicher, S. Soff, and X. Zhu, preprint nucl-th/0412022.

[14] H. Liu, S. Panitkin, and N. Xu, Phys. Rev. C 59 (1999) 348.

[15] R.J.M. Snellings et al., Phys. Rev. Lett. 84 (2000) 2803.

[16] W. Cassing, K. Gallmeister, and C. Greiner, Nucl. Phys. A 735 (2004) 277.

[17] Z.W. Lin and C.M. Ko, Phys. Rev. C 65 (2002) 034904.

[18] Z.W. Lin, C.M. Ko, B.A. Li, B. Zhang, and S. Pal, preprint nucl-th/0411110.

[19] L.V. Bravina et al., Phys. Lett. B 354 (1995) 196; L.V. Bravina, I.N. Mishustin, and J.P. Bondorf, Nucl. Phys. A 594 (1995) 425.

[20] L.V. Bravina et al., Phys. Rev. C 60 (1999) 044905; Heavy Ion Phys. 5 (1997) 455.

[21] H. Sorge, Phys. Lett B 373 (1996) 16; R. Mattiello, H. Sorge, H. Stöcker, and W. Greiner, Phys. Rev. C 55 (1997) 1443.

[22] S.A. Bass et al., Prog. Part. Nucl. Phys. 41 (1998) 255.

[23] L.D. Landau, Izv. Akad. Nauk SSSR 17 (1953) 51.

[24] V. Gribov, Sov. Phys. JETP 26 (1968) 414; L.V. Gribov, E.M. Levin, and M.G. Ryskin, Phys. Rep. 100 (1983) 1.

[25] A.B. Kaidalov and K.A. Ter-Martirosian, Phys. Lett. B 117 (1982) 247; A.B. Kaidalov, Surveys in High Energy Phys. 13 (1999) 265.

[26] N.S. Amelin et al., Sov. J. Nucl. Phys. 50 (1989) 1058; Phys. Rev. C 47 (1993) 2299; N.S. Amelin and L.V. Bravina, Sov. J. Nucl. Phys. 51 (1990) 211; *ibid.* 51 (1990) 133.

[27] S. Donnachie, G. Dosch, O. Nachtmann, and P. Landshoff, Pomeron Physics and QCD (Cambridge, Cambridge, 2002).

[28] V. Barone and E. Predazzi, High-Energy Particle Diffraction (Springer, Heidelberg, 2002).

[29] H.J. Drescher et al., Phys. Rep. 350 (2001) 93.

[30] L. McLerran, Lectures on Quark Matter, edited by W. Plessas and L. Mathelitsch (Springer, Heidelberg, 2001), p. 291.

[31] I.P. Lokhtin, S.V. Petrushanko, L.I. Sarycheva, and A.M. Snigirev, Pramana 60 (2002) 1045.

[32] L. Bravina et al., J. Phys. G 28 (2002) 1977; Phys. Lett. B 543 (2002) 217; Nucl. Phys. A 715 (2003) 665c.

[33] E. Zabrodin, L. Bravina, C. Fuchs, and A. Faessler, Prog. Part. Nucl. Phys. 53 (2004) 183.

[34] G. Burau et al., preprint nucl-th/0411117.

[35] M.B. Tonjes et al., PHOBOS collaboration, J. Phys. G 30 (2004) 1243; B. Back et al., PHOBOS collaboration, preprint nucl-ex/0407012.

[36] N. Borghini, P.M. Dinh, and J.-Y. Ollitrault, Phys. Rev. C 64 (2001) 054901; N. Borghini, R.S. Bhalerao, and J.-Y. Ollitrault, J. Phys. G 30 (2004) 1213.